



**HAL**  
open science

## Single reaction mixture synthesis and characterization of CoF<sub>2</sub>O<sub>4</sub> – BaFe<sub>12</sub>O<sub>19</sub> nano-composite

Saurabh Raghuvanshi, Priyanka Tiwari, Rulan Verma, Arindam Ghosh,  
Frédéric Mazaleyrat, Shashank Kane

► **To cite this version:**

Saurabh Raghuvanshi, Priyanka Tiwari, Rulan Verma, Arindam Ghosh, Frédéric Mazaleyrat, et al.. Single reaction mixture synthesis and characterization of CoF<sub>2</sub>O<sub>4</sub> – BaFe<sub>12</sub>O<sub>19</sub> nano-composite. Advances in basic Science (ICABS 2019), Feb 2019, Bahal, India. pp.070031, 10.1063/1.5122423 . hal-04453061

**HAL Id: hal-04453061**

**<https://hal.science/hal-04453061>**

Submitted on 12 Feb 2024

**HAL** is a multi-disciplinary open access archive for the deposit and dissemination of scientific research documents, whether they are published or not. The documents may come from teaching and research institutions in France or abroad, or from public or private research centers.

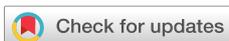
L'archive ouverte pluridisciplinaire **HAL**, est destinée au dépôt et à la diffusion de documents scientifiques de niveau recherche, publiés ou non, émanant des établissements d'enseignement et de recherche français ou étrangers, des laboratoires publics ou privés.

Copyright

RESEARCH ARTICLE | AUGUST 29 2019

# Single reaction mixture synthesis and characterization of $\text{CoF}_2\text{O}_4 - \text{BaFe}_{12}\text{O}_{19}$ nano-composite

S. Raghuvanshi; P. Tiwari; R. Verma; A. Ghosh; F. Mazaleyrat; S. N. Kane 



AIP Conf. Proc. 2142, 070031 (2019)

<https://doi.org/10.1063/1.5122423>



CrossMark



Cut Hall measurement time in *half* using an M91 FastHall™ controller



Also available as part of a tabletop system and an option for your PPMS® system

# Single Reaction Mixture Synthesis And Characterization Of $\text{CoFe}_2\text{O}_4 - \text{BaFe}_{12}\text{O}_{19}$ Nano-composite

S. Raghuvanshi<sup>1</sup>, P. Tiwari<sup>1,2</sup>, R. Verma<sup>1</sup>, A. Ghosh<sup>3</sup>, F. Mazaleyrat<sup>4</sup> and S. N. Kane<sup>1, a)</sup>

<sup>1</sup>Magnetic Materials Laboratory, School of Physics, D. A. University, Indore-452001, India.

<sup>2</sup>Department of Physics, Prestige Institute of Engineering Management and Research, Indore-452010, India.

<sup>3</sup>Department of Physics, GDC Memorial College, Bahal (Bhiwani) Haryana, India.

<sup>4</sup>SATIE, ENS Cachan, CNRS 8029, Universite Paris-Saclay, 61 Av. du Pdt. Wilson, F-94230, Cachan, France.

<sup>a)</sup>Corresponding author: kane\_sn@yahoo.com

**Abstract.**  $(\text{CoFe}_2\text{O}_4)_x(\text{BaFe}_{12}\text{O}_{19})_{1-x}$  ( $x = 0.0, 0.4, 0.6, 0.8, 1.0$ ) nano-composites was synthesized via single reaction mixture, utilizing sol-gel auto combustion method, with an intention to have superior structural homogeneity, and eventually to have single magnetic phase with enhanced exchange coupling between  $\text{CoFe}_2\text{O}_4$  (*soft*) –  $\text{BaFe}_{12}\text{O}_{19}$  (*hard*) phase. As-synthesized composite was thermally treated at 800 °C/4hrs, needed for the formation of hexagonal phase. X-ray diffraction (XRD) displays presence of both soft and hard phases only. Grain size for  $\text{BaFe}_{12}\text{O}_{19}$  and  $\text{CoFe}_2\text{O}_4$  respectively range between 50.2 – 54.5 nm and 45.5 – 56.5 nm. Obtained value of saturation magnetization ( $M_s$ ), coercivity ( $H_c$ ) for the studied samples is respectively: 39.8 Am<sup>2</sup>/kg – 75.5 Am<sup>2</sup>/kg and 501.2 Oe – 2587.9 Oe. Observed  $M_s$ ,  $H_c$  values clearly show that single reaction mixture leads to better exchange coupling between soft-hard phases.  $M_s$  enhancement was also observed with increasing substitution amount ( $x$ ). Observed results point out  $(\text{CoFe}_2\text{O}_4)_x(\text{BaFe}_{12}\text{O}_{19})_{1-x}$  composite system as a good candidate for their potential applications as hard magnets.

## INTRODUCTION

The curiosity of research and development in the field of nano-crystalline magnetic materials has been escalating both from fundamental physics and technological application, as these materials display many distinctive and remarkable physical and chemical properties. Nano-composite materials that constitute fine mixture of hard, soft magnetic phases demonstrate enhanced properties which make them appropriate for various applications e. g. - advanced recording applications, video recorders, microwave-absorbing materials, permanent magnets [1-4]. In addition to the size, shape, exchange coupling interaction, distribution of cation as well as constituent grains, and dipolar interaction also play a vital role in magnetic properties of a two phase (soft-hard) magnetic nano composite [5]. M-type barium hexaferrite ( $\text{BaFe}_{12}\text{O}_{19}$ ) is a well known high performance permanent magnetic material, due to its reasonably high Curie temperature, large magneto-crystalline anisotropy, moderately large saturation magnetization, admirable chemical stability, and corrosion resistivity [6-7]. Spinel cobalt ferrite ( $\text{CoFe}_2\text{O}_4$ ) has attracted enormous concern owing to its noteworthy properties such as significant thermal, and chemical stabilities, high saturation magnetization ( $M_s$ ), and good mechanical hardness. They have been extensively applied in various fields, including magnetic resonance imaging, magnetically targeted drug delivery, permanent magnets, microwave absorption, and magnetic data storage [8-11]. The magnetic characteristics of nano composite are strongly affected when the size of particle move towards the critical diameter, below which each particle is a single magnetic domain. Synthesis methods play a crucial role for controlling structural parameter of nano-composite. Majority of preparation methods available in literature for the synthesis of nano-composites start with mixing hard, soft phases and afterward exchange couple either via electroplating [12], chemical [13], ball-milling [14] or heat-treatment [15]. In order to get better exchange coupling, there is a serious need of high level of homogenous mixing of hard-soft

ferrite phase [16], which is better ensured if the growth of both of these phases takes place together from a single reaction mixture.

Therefore, in the present work we report single reaction mixture synthesis, structural and magnetic characterization of  $(\text{CoFe}_2\text{O}_4)_x(\text{BaFe}_{12}\text{O}_{19})_{1-x}$  soft-hard nano-composite, to get better structural homogeneity and to be able to achieve improved exchange coupling between both the phases, leading to superior magnetic properties.

## EXPERIMENTAL DETAILS AND DATA ANALYSIS

Nano-composites having nominal composition  $(\text{CoFe}_2\text{O}_4)_x(\text{BaFe}_{12}\text{O}_{19})_{1-x}$  ( $x = 0.0, 0.4, 0.6, 0.8, 1.0$ ) were prepared by single reaction mixture via sol-gel auto combustion method, utilizing nitrate-citrate precursors. All the pre-cursors (keeping metal salt-fuel mass ratio = 1:1) were mixed in 10 ml de-ionized water, keeping pH 7 by adding ammonia ( $\text{NH}_4\text{OH}$ ) solution. Citric acid was used as fuel. Obtained clear solution was then heated at  $\sim 120^\circ\text{C}$  in air till fluffy powder was formed called as 'dry gel' or 'as-burnt powder', which was heated at  $800^\circ\text{C}$  for 4 hours. X-ray diffraction (XRD) measurements were done at room temperature by using Bruker D8 advance diffractometer with  $\text{CuK}_\alpha$  radiation ( $\lambda = 0.15406\text{ nm}$ ). The XRD patterns were recorded in the angular range  $10^\circ \leq 2\theta \leq 90^\circ$  with a step size of  $0.02^\circ$ . XRD data was analyzed to obtain structural information in the studied samples. Hysteresis measurements were done by utilizing Lakeshore Model 7410 vibration sample magnetometer (VSM) (maximum field –  $H_{\text{max}} \approx \pm 1.8$  Tesla), to obtain coercivity ( $H_c$ ), remanence ( $M_r$ ), saturation magnetization ( $M_s$ ) and squareness ratio or reduced remanent magnetization ( $M_r/M_s$ ). Experimental lattice parameter ( $a, c$ ) for hexagonal phase ( $\text{BaFe}_{12}\text{O}_{19}$ ) was calculated by analyzing XRD data as described in [17]. Cell volume ( $V$ ) of hexagonal phase of the studied samples was determine by using the equation  $V = 0.8666 \times a^2 \times c$ , where  $a, c$  - experimental lattice parameters of hexagonal phase. Grain diameter for cubic phase was obtained by the line width of [311] reflection, using Scherrer's formula:  $D_s = 0.9\lambda / \beta \cos\theta$ , Where  $\lambda$  - wavelength of the x-ray used,  $\beta$  - line width,  $\theta$  peak position (in  $2\theta$  scale).

## RESULTS AND DISCUSSION

XRD patterns as a function of substitution amount of the studied nano-composite samples are shown in Fig. 1a.

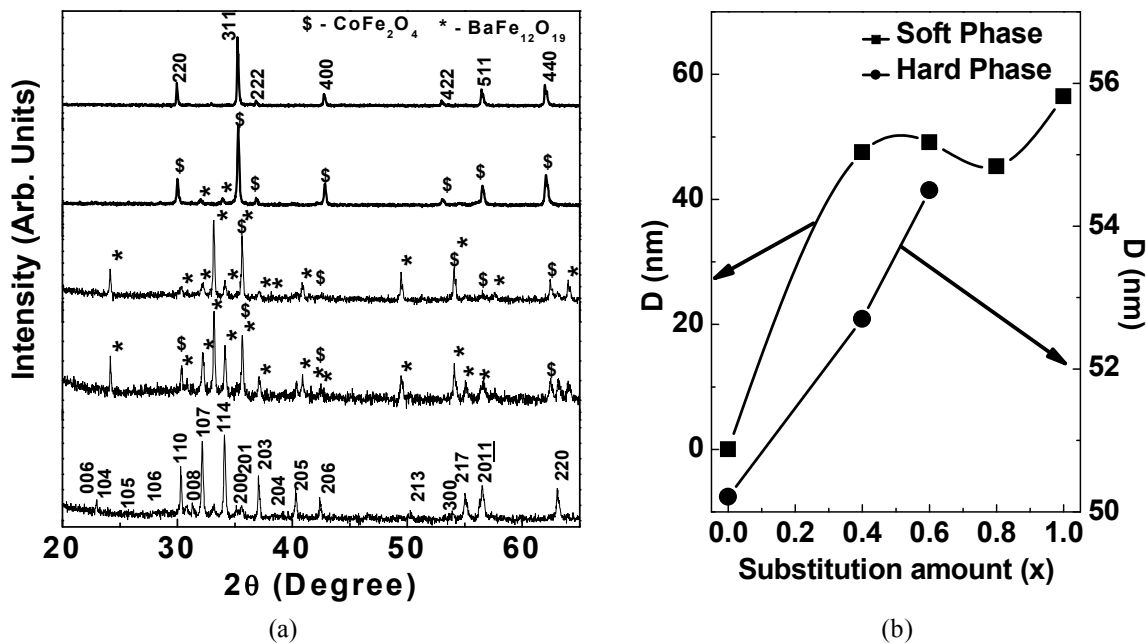


FIGURE 1. (a) X-ray diffraction patterns of  $\text{CoFe}_2\text{O}_4/\text{SrFe}_{12}\text{O}_{19}$  nano-composite. (b) Variation of grain size of cubic phase, and hexagonal phase with substitution amount. (Line connecting points is guide to the eye)

**TABLE 1.** Lattice parameter ( $a$ ,  $c$ ), unit cell volume ( $V$ ), hopping length for tetrahedral and octahedral sites ( $L_A$ ,  $L_B$ ) of  $\text{CoFe}_2\text{O}_4/\text{BaFe}_{12}\text{O}_{19}$  nano-composite.

x	Phase		Lattice Parameter (nm)	V (nm <sup>3</sup> )	L <sub>A</sub> (nm)	L <sub>B</sub> (nm)
0.0	Hexagonal	(BaFe <sub>12</sub> O <sub>19</sub> ) <sub>1.0</sub>	a= 0.5892, c=2.3211	0.6983	–	–
0.4	Hexagonal	(BaFe <sub>12</sub> O <sub>19</sub> ) <sub>0.6</sub>	a=0.5958, c=2.2138	0.6810	–	–
	Cubic	(CoFe <sub>2</sub> O <sub>4</sub> ) <sub>0.4</sub>	a=0.8346	0.5813	0.3614	0.2954
0.6	Hexagonal	(BaFe <sub>12</sub> O <sub>19</sub> ) <sub>0.4</sub>	a=0.5958, c=2.0485	0.6302	–	–
	Cubic	(CoFe <sub>2</sub> O <sub>4</sub> ) <sub>0.6</sub>	a=0.8349	0.5821	0.3615	0.2956
0.8	Hexagonal	(BaFe <sub>12</sub> O <sub>19</sub> ) <sub>0.2</sub>	–	–	–	–
	Cubic	(CoFe <sub>2</sub> O <sub>4</sub> ) <sub>0.8</sub>	a=0.8359	0.5841	0.3619	0.2959
1.0	Cubic	(CoFe <sub>2</sub> O <sub>4</sub> ) <sub>1.0</sub>	a=0.8369	0.5863	0.3624	0.2963

By examining XRD patterns it is observed that all the investigated samples show presence of cubic spinel  $\text{CoFe}_2\text{O}_4$  (S) phase, hexagonal  $\text{SrFe}_{12}\text{O}_{19}$  (\*) phase, and no other secondary phase is formed. Figure 1b illustrates variation of grain size ( $D$ ) for both cubic, hexagonal phases. Grain diameter ( $D$ ) of the studied samples show minor changes with increasing substitution amount (Fig. 1 b), range between 50.2 nm to 54.5 nm for hexagonal phase and 45.5 nm to 56.5 nm for cubic phase suggests, that changes in substitution amount leads to particle agglomeration.

Substitution amount dependence of lattice parameter ( $a$ ,  $c$ ), unit cell volume ( $V$ ) for hexagonal, cubic phases and hopping length for tetrahedral and octahedral sites ( $L_A$ ,  $L_B$ ) for cubic phase of the prepared nano-composites are depicted in table 1. Observed changes in lattice parameter ( $a$ ,  $c$ ) with increasing substitution amount is ascribed to the replacement of elements having different ionic radii. Obtained values of lattice parameter ( $a$ ) for hexagonal and cubic phases respectively range between 0.5892 nm – 0.5958 nm and 0.8346 nm – 0.8369 nm, validates the formation of hexagonal, and cubic (*spinel*) phase. The hopping length (distance between the magnetic ions) for tetrahedral ( $L_A$ ) and octahedral ( $L_B$ ) site and cell volume ( $V$ ) follows same trend as that of lattice parameter ( $a$ ) of cubic phase, illustrates increase with substitution amount.

Figure 2a displays compositional dependent variation of saturation magnetization ( $M_s$ ), whereas inset of Fig. 2a gives coercivity ( $H_c$ ) of the studied samples. Figure 2b shows hysteresis loops of the studied hard soft nano-composite (inset illustrates magnified view of the hysteresis loop to show changes in magnetization).

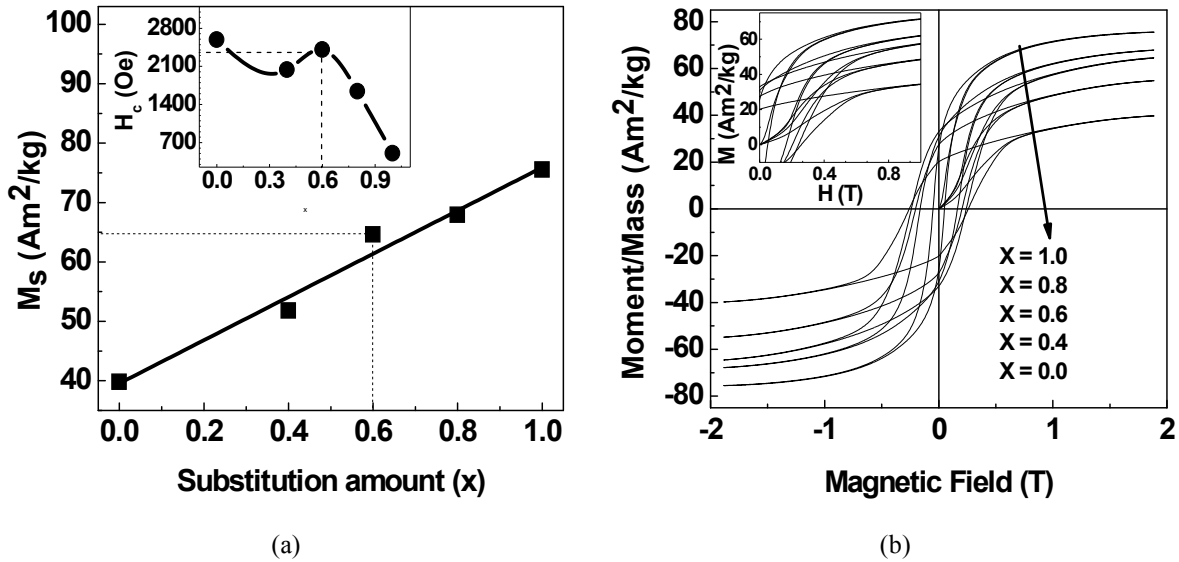


**FIGURE 2.** (a) Composition dependent saturation magnetization ( $M_s$ ) at 300K. Line connecting points is linear fit to the data, Inset: Variation of coercivity ( $H_c$ ) with substitution amount. Line connecting points is guide to the eye. (b) Hysteresis loops (Inset: magnified view of hysteresis loops) of  $\text{CoFe}_2\text{O}_4/\text{BaFe}_{12}\text{O}_{19}$  nano-composite

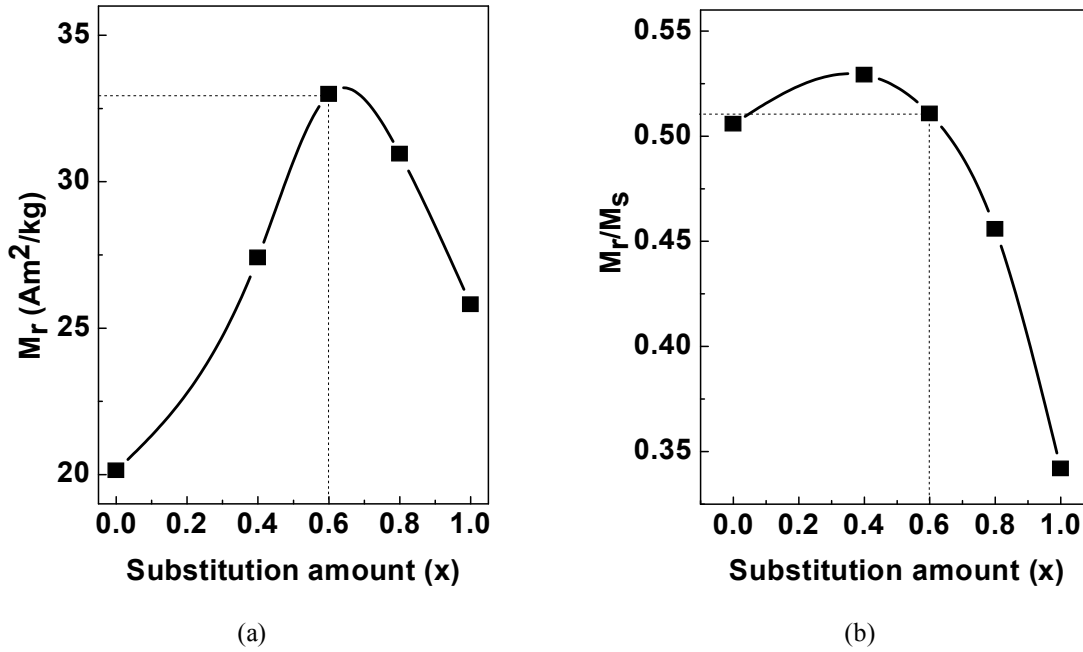


**FIGURE 3.** Composition dependent (a) remanence ( $M_r$ ), and (b) squareness ratio ( $M_r/M_s$ ) of studied  $\text{CoFe}_2\text{O}_4/\text{BaFe}_{12}\text{O}_{19}$  nano-composite. Line connecting points is guide to the eye.

It is worth noting that the exchange interaction, and dipolar interaction plays a key role in determining magnetic properties of the magnetic nano-composite materials. Generally three different types of exchange interaction formed at the interface between hard-hard, soft-soft, and soft-hard grains, which has been proposed by Han et al. in 2004 [18]. The sufficient exchange coupling will not only display the magnetization in the  $\text{CoFe}_2\text{O}_4$  grains but also make the magnetic moments of the interface of the  $\text{CoFe}_2\text{O}_4/\text{BaFe}_{12}\text{O}_{19}$  nano-composite opposing from the local easy axis and aligning parallel to each other, which leads to a higher value of the  $M_s$  [17], as was also observed in present work.

Perusal of Fig. 2b reveals good single phase magnetic behavior of the studied samples. Observed smooth change in magnetization as a function of applied field exhibits a single magnetic phase, ascribed to stronger exchange coupling between hexagonal (*hard*) - cubic (*soft*) magnetic phases. Obtained value of saturation magnetization and coercivity for the studied samples ranges between  $39.8 \text{ Am}^2/\text{kg} - 75.5 \text{ Am}^2/\text{kg}$  and  $501.2 \text{ Oe} - 2587.9 \text{ Oe}$  respectively, suggests substitution amount ( $x$ ) enhances both  $M_s$  and  $H_c$ .

Compositional dependence of changes in remanence ( $M_r$ ), and squareness ratio ( $M_r/M_s$ ) are depicted in Fig. 3a, b. Perusal of Fig. 3a shows initially  $M_r$  increases upto  $x = 0.0 - 0.6$ , than for higher value of substitution amount its value decreases. Observed decrease in  $M_r/M_s$  ratio with increasing substitution amount (see Fig. 3b), reveals for higher  $x$  values (substitution amount) softer nature of studied nano-composite. Results clearly illustrate,  $x = 0.6$  (marked by dashed line in Fig. 2a, 3a, b) is optimum composition to have improved  $H_c$  ( $2405.9 \text{ Oe}$ ),  $M_r$  ( $32.9 \text{ Am}^2/\text{kg}$ ),  $M_r/M_s$  ( $0.51$ ) as well as  $M_s$  ( $64.6 \text{ Am}^2/\text{kg}$ ), reveals best composition to be used in hard magnetic applications.

## SUMMARY

We have presented a single reaction mixture synthesis of  $\text{BaFe}_{12}\text{O}_{19}/\text{CoFe}_2\text{O}_4$  exchange coupled nano-composite and its characterization using XRD, VSM techniques. XRD confirms the presence of both hexagonal (*hard*), cubic spinel (*soft*) phases, no other secondary phase is formed. Obtained values of lattice parameter ( $a$ ) for hexagonal, cubic phases validate the formation of hexagonal and cubic (*spinel*) phase. The magnetization of nano-composites demonstrates hysteresis loops, characteristic of an exchange coupled system showing single magnetic phase, although XRD validates the presence of two phases (cubic, hexagonal). Good exchange coupling, between  $\text{CoFe}_2\text{O}_4$ ,

and BaFe<sub>12</sub>O<sub>19</sub> ferrite, results in enhanced saturation magnetization (75.5 Am<sup>2</sup>/kg), and remanence (20.1 Am<sup>2</sup>/kg) as compared to pure BaFe<sub>12</sub>O<sub>19</sub> (shown as  $M_s = 39.8 \text{ Am}^2/\text{kg}$ ,  $M_r = 39.8 \text{ Am}^2/\text{kg}$ ). Present studies clearly show that, via single reaction mixture synthesis and using appropriate substitution amount, one can get enhanced magnetic properties for various applications.

## ACKNOWLEDGMENTS

Authors thank Dr. M. Gupta, Mr. L. Behra, UGC-DAE CSR, Indore for XRD measurements. This work is financially supported by UGC-DAE CSR Projects: CSR-IC/CRS-149/2015-16/06. Research fellowship to SR from UGC-DAE CSR Project No. CSR-IC/CRS-74/2014-15/2104 is gratefully acknowledged.

## REFERENCES

1. M. H. Kryder, *MRS Bull.* **21**, 17–19 (1996).
2. A. Manaf, R. A. Buckley and H. A. Davies, *J. Magn. Magn. Mater.* **128**, 302–306 (1993).
3. L. Withanawasam, G. C. Hadjipanayis and R.F. Krause, *J. Appl. Phys.* **75**, 6646–6648 (1994).
4. Y. Zhu, L. P. Stubbs and F. Ho, *Chem. Cat. Chem.* **2**, 365–374 (2010).
5. K. P. Remya, D. Prabhu, S. Amirthapandian, C. Viswanathan and N. Ponpandian, *J. Magn. Magn. Mater.* **406**, 233–238 (2016).
6. N. Yang, H. B. Yang, J. J. Jia and X. F. Pang, *J. Alloys Comp.* **438**, 263–267 (2007).
7. S. Diaz-Castanon, J. L. Sanchez, L. I. Estevez-Rams, F. Leccabue and B. E. Watts, *J. Magn. Magn. Mater.* **185**, 194–198 (1998).
8. Y. Wang, D. Su, A. Ung, J. H. Ahn, G. Wang, *Nanotechnology* **23**, 305501–7 (2012).
9. A. Lopez-Ortega, M. Estrader, G. A. Alvarez, A. G. Roca, J. Nogues, *Phys Rep.* **553**, 1–32 (2015).
10. R. Rakshit, M. Mandal, M. Pal, K. Mandal, *Appl. Phys. Lett.* **104**, 092412–0912417 (2014).
11. D. Mazuera, O. Perales, M. Suarez, S. Singh, *Mater. Sci. Eng. A* **527**, 6393–9 (2010).
12. Q. Zeng, Y. Zhang, M. J. Bonder, and G. C. Hadjipanayis, *J. Appl. Phys.* **93**, 6498–6500 (2003).
13. J. H. Hong, W. S. Kim, J. I. Lee, and N. H. Hur, *J. Solid. State Commun.* **141**, 541 (2007).
14. J. Ding, P. G. McCormick, and R. Street, *J. Magn. Magn. Mater.* **124**, 1–4 (1993).
15. J. M. Le Breton, R. Larde, H. Chiron, V. Pop, D. Givord, O. Isnard, and I. Chichinas, *J. Phys. D: Appl. Phys.* **43**, 085001 (2010).
16. D. Neupane, M. Ghimire, H. Adhikari, A. Lisfi, and S. R. Mishra, *AIP Advances* **7**, 055602-1–11 (2017).
17. L. Pan, D. Cao, P. Jing, J. Wang and Q. Liu, *Nanoscale Res. Lett.* **10:131**, 1–7 (2015)
18. G. B. Han, R. W. Gao, S. Fu, W. C. Feng, H. Q. Liu, W. Chen, W. Li, Y. Q. Guo, *Appl Phys A* **81**, 579–582 (2004).